WIND ENERGY
*Wind Energ.* 2010; **13**:587–602
Published online 9 December 2009 in Wiley Online Library (wileyonlinelibrary.com). DOI: 10.1002/we.379

RESEARCH ARTICLE

# Simulation of wind turbine wake interaction using the vorticity transport model

Timothy M. Fletcher and Richard E. Brown

Rotor Aeromechanics Laboratory, Department of Aerospace Engineering, University of Glasgow, Glasgow, G12 8QQ, United Kingdom

## ABSTRACT

The aerodynamic interactions that can occur within a wind farm can result in the constituent turbines generating a lower power output than would be possible if each of the turbines were operated in isolation. Tightening of the constraints on the siting of wind farms is likely to increase the scale of the problem in the future. The aerodynamic performance of turbine rotors and the mechanisms that couple the fluid dynamics of multiple rotors can be most readily understood by simplifying the problem and considering the interaction between only two rotors. The aerodynamic interaction between two rotors in both co-axial and offset configurations has been simulated using the Vorticity Transport Model. The aerodynamic interaction is a function of the tip speed ratio, and both the streamwise and crosswind separation between the rotors. The simulations show that the momentum deficit at a turbine operating within the wake developed by the rotor of a second turbine is governed by the development of instabilities within the wake of the upwind rotor, and the ensuing structure of the wake as it impinges on the downwind rotor. If the wind farm configuration or wind conditions are such that a turbine rotor is subject to partial impingement by the wake produced by an upstream turbine, then significant unsteadiness in the aerodynamic loading on the rotor blades of the downwind turbine can result, and this unsteadiness can have considerable implications for the fatigue life of the blade structure and rotor hub. Copyright © 2009 John Wiley & Sons, Ltd.

**KEYWORDS**
wake instability; interaction; wind turbine; VTM

**Correspondence**
T. Fletcher, Rotor Aeromechanics Laboratory, Department of Aerospace Engineering, University of Glasgow, Glasgow, G12 8QQ, United Kingdom.
E-mail: t.fletcher@eng.gla.ac.uk

Received 16 April 2009; Revised 1 September 2009; Accepted 20 October 2009

## NOMENCLATURE

| | |
|---|---|
| $A$ | rotor disc area |
| $C_n$ | normal force coefficient, $F_n \Big/ \frac{1}{2}\rho c\left(V_\infty^2 + (\Omega r)^2\right)$ |
| $C_P$ | rotor power coefficient, $P \Big/ \frac{1}{2}\rho A V_\infty^3$ |
| $C_t$ | tangential force coefficient, $F_t \Big/ \frac{1}{2}\rho c\left(V_\infty^2 + (\Omega r)^2\right)$ |
| $C_T$ | rotor thrust coefficient, $T \Big/ \frac{1}{2}\rho A V_\infty^2$ |
| $F_n$ | sectional normal force |
| $F_t$ | sectional tangential force (+ve forward) |
| $Q$ | low speed shaft torque |
| $R$ | rotor radius |
| $r$ | radial location |
| $S$ | vorticity source |
| $u$ | flow velocity |
| $u_b$ | flow velocity relative to blade |
| $V_\infty$ | wind velocity |
| $x_h$, $y_h$ | downwind and crosswind spacing |
| $\alpha$ | angle of attack |
| $\lambda$ | tip speed ratio, $\Omega R/V_\infty$ |
| $\nu$ | kinematic viscosity |
| $\rho$ | density |
| $\Omega$ | rotational speed |
| $\omega$ | vorticity |
| $\omega_b$ | bound vorticity |
| $\psi$ | rotor azimuth |

Copyright © 2009 John Wiley & Sons, Ltd.

## ABBREVIATIONS

| | |
|---|---|
| Ref | reference rotor |
| DW | downwind rotor |

## 1. INTRODUCTION

The aerodynamic interactions between the constituent turbines of a wind farm have been known for some time to degrade its overall power output (see the survey papers by Vermeer, Sørensen and Crespo,[1] and Crespo, Hernández and Frandsen[2]). The interaction is principally a result of the impingement of the wakes developed by the turbines, and thus may be exacerbated by the configuration of the turbines within the farm. A wake is developed by a wind turbine rotor as a consequence of the turbine generating lift and drag forces, and results in a momentum deficit downwind of the turbine. At the typical design conditions at which horizontal axis wind turbines are operated, the wind speed is high enough relative to the tip speed of the rotor for the vortical structures that form its wake to be convected many rotor radii downwind without significant viscous dissipation. Any turbines located downwind that become immersed within this wake will experience a reduction in the energy within their incident flow, and thus, a reduction in their power output. The separation between the turbines in wind farms can vary significantly, particularly at onshore sites where the size of installations is constrained by the shortage of suitable ground for the turbine foundations. As indicative examples, the turbines in the onshore wind farm at West Kilbride in Scotland are spaced approximately 10 rotor radii apart, whilst those at the offshore Horns Rev wind farm in Danish waters are separated by a distance of 14 rotor radii. In practice, the distribution of the turbines within wind farms is designed to minimize, where possible, the interaction between the turbines under prevailing wind conditions.

The major constraints imposed on the overall area that may be occupied by an onshore wind farm include the topography of the chosen site. Offshore wind farms are subject to different but equally significant constraints, such as the need not to impose unduly on shipping lanes. Significant interest in understanding the aerodynamic interactions within wind farms has developed over the last 30 years in order to allow the optimization of wind farm configurations and to permit increases in turbine density. Newman[3] used a theoretical approach that accounted for different types of surface topography to show that significant power losses would occur if the turbine spacing was too low. In 1978, Builtjes and Smit[4] investigated the optimal spacing of vertical axis wind turbines using a combination of wind tunnel data and numerical methods, indicating that as the number of turbines within the farm is increased, so should the spacing between the turbines in order to achieve optimal power output. Lissaman[5] developed a numerical model to predict the power degradation in wind turbine arrays using momentum conservation and reduced-order models for wake growth and ground effect. Milborrow[6] used a combination of experimental and analytical methods to investigate the effects of interaction between wind turbines on the overall efficiency of a farm. It was estimated that the power output from a typical wind farm, as envisaged at that time, could be 25% lower than that of an equivalent number of turbines operating in isolation.

Sforza, Sheerin and Smorto[7] developed a model in which the wakes induced by the wind turbine rotors were treated as small perturbations to a uniform freestream. Results from this model were then compared with the velocity measured at various downwind locations during wind tunnel tests. Sforza, Sheerin and Smorto found good agreement between theoretical predictions of the velocity deficit downwind of a given turbine rotor and experimental measurements. Voutsinas, Rados and Zervos[8] developed an effective means of modelling the annual energy output of arrays of large numbers of turbines using the Abramovich theory of turbulent jets. Voutsinas and his co-workers concluded that the simplified modelling of the individual turbines in this case was not able to fully represent all of the pertinent physics in the development of the flow, and that to understand better the energy extraction process, a more physically realistic representation of the wake of each wind turbine would be required. The literature described above is intended as a sample of the many efforts that have been made towards producing simplified models of wind turbine wakes and the effects of aerodynamic interactions within wind farms. Unfortunately, simplified models of the mean velocity deficit downstream of wind turbines are of very limited use when validating models based on the solution of the Navier-Stokes equations, particularly those that are explicitly designed to capture the complex vortical structure and unsteadiness within the wakes developed by wind turbines. This problem exists even when the effects of atmospheric turbulence, wind shear and tower shadow are included within the simplified model. The pan-European UpWind project[9] has been conducted, in part, to improve the modelling of the flow within large offshore wind farms and to provide better predictions of power production, principally by bridging the gap between conventional computational fluid dynamics (CFD) methods and those models of entire wind farms that typically incorporate very simple wake models. Recent developments in the simulation of wind turbine wakes include the use of large-eddy simulation coupled to an actuator line model for the aerodynamic loading on the blades, such as the calculations performed by Troldborg, Sørensen and Mikkelson.[10]

In this paper, a computational model that solves the incompressible Navier-Stokes equation in vorticity–velocity form will be introduced, and then applied to a series of simplified wind farm interactions. By solving the governing equations of fluid motion in vorticity–velocity form, some of the inherent problems of numerical dissipation that are encountered when solving the Navier-Stokes equa-


*Wind Energ.* 2010; **13**:587–602 © 2009 John Wiley & Sons, Ltd.
DOI: 10.1002/we

tions in pressure–velocity–density form may be avoided. By providing a high-fidelity representation of the structure and evolution of the wake of a wind turbine rotor and its interaction with other turbines within a wind farm, the fluid dynamics associated with the power losses discussed above can be better understood. In particular, the important role of wake instability in governing the momentum deficit downwind of a wind turbine can be understood better. Importantly, this may allow the designers of wind farms to explore ways in which to alleviate the adverse effects of interaction, including not only power losses, but also the unsteady loads that can result in unnecessary fatigue of the components within the hub and transmission system. Any strategy for the active optimization of wind farm performance using individual turbine control, or passive alleviation of wake effects, will require a detailed characterization of the velocity that is induced at the blades of each individual turbine by the wakes of other turbines. The approach that is presented in this paper, through providing an accurate and detailed model of the flow physics that are associated with the interactions between individual turbines, may contribute to the development of effective strategies for either the active or passive control of turbine blades in order to allow the power losses within wind farms to be mitigated.

## 2. COMPUTATIONAL AERODYNAMICS

The aerodynamic performance of two generic horizontal axis wind turbine rotors and their fluid dynamic interaction has been simulated in a number of representative configurations using the Vorticity Transport Model (VTM) developed by Brown,[11] and extended by Brown and Line.[12] The VTM enables the simulation of wind turbine aerodynamics and performance using a high-fidelity model of the wake generated by the turbine rotor. The VTM solves the vorticity transport equation in finite-volume form using a structured Cartesian mesh within the domain surrounding the turbine rotor. The vorticity transport equation is obtained by making the physically realistic assumption of incompressibility within the wake, and then casting the Navier-Stokes equations into the vorticity-velocity form

$$\frac{\partial}{\partial t}\omega + u\cdot\nabla\omega - \omega\cdot\nabla u = S + \upsilon\nabla^2\omega \qquad (1)$$

The advection, stretching and diffusion terms within the vorticity transport equation describe the changes in the vorticity field, $\omega$, with time at any point in space, as a function of the velocity field, $u$, and the viscosity, $\nu$. The physical condition that vorticity may neither be created nor destroyed within the flow, and thus may only be created at the solid surfaces immersed within the fluid, is accounted for using the vorticity source term, $S$. The vorticity source term is determined as the sum of the temporal and spatial variations in the bound vorticity, $\omega_b$, on the turbine blades:

$$S = -\frac{d}{dt}\omega_b + u_b\nabla\cdot\omega_b \qquad (2)$$

The bound vorticity distribution on the blades of the rotor is modelled using an extension of lifting-line theory. The velocity field is related to the vorticity field by using a Cartesian fast multipole method to invert the differential form of the Biot-Savart law

$$\nabla^2 u = -\nabla\times\omega. \qquad (3)$$

Mass conservation is achieved to numerical accuracy by using a kernel within the fast multipole method that is divergence-free. Use of the fast multipole method to invert equation (3), in conjunction with an adaptive grid in which cells are only present within the calculation when the vorticity within them is non-zero, dramatically increases the computational efficiency of the scheme when compared to an equivalent calculation performed on a fixed grid. In the current analysis, the ground plane is not modelled and, therefore, the velocity gradient associated with the atmospheric boundary layer does not influence the flow field surrounding the turbines. In order to better understand the effect of wake instability on the characteristics of the flow downwind of turbines, the turbulence that is normally present within the atmosphere was also not modelled. The method is rendered effectively boundary-free as cells may be created, when necessary, on a Cartesian stencil that extends to infinity, using the assumption that there is zero vorticity outside the wake.[12] An assumption is made that the Reynolds number within the computational domain is sufficiently high that the governing flow equation may be solved in inviscid form. Dissipation of the wake does still occur, however, through the mechanism of natural vortical instability. The numerical diffusion of vorticity within the flow field surrounding the wind turbines is kept at a very low level by using a Riemann problem technique based on the Weighted Average Flux method developed by Toro[13] to advance equation (1) through time. This approach allows highly efficient multi-rotor simulations, and permits many rotor revolutions to be captured without significant spatial smearing of the wake structure. This is in contrast to the performance of more conventional CFD techniques based on the pressure–velocity–density formulation of the Navier-Stokes equations.

The VTM has been used successfully to investigate the aerodynamic interaction between the main and tail rotors of a helicopter,[14] and for the study of helicopter main rotor—fuselage interaction.[15] It has also been used to model the performance of rotors in axial flight[16] and to examine the fluid dynamics of the rotor vortex ring state.[17] Notably, it has also been validated against experimental data for co-axial helicopter rotors.[18]

## 3. WIND TURBINE MODEL

The rotor model that was used for the present study is a three-bladed version of the rotor used for Phase VI of the NREL Unsteady Aerodynamics Experiment.[19] Three blades were used in order to better represent the wind turbine rotors that are used within most modern wind farms. The addition of the third blade increases the solidity of the rotor and, therefore, the rotor power coefficient at low tip speed ratios, such that the peak performance of the rotor occurs at tip speed ratios in the range 6–8. The structural deformation of the blades, in the form of bending, torsion and extension, are not modelled in the current analysis, and the blades are attached rigidly to the hub. In addition, the aerodynamic effects associated with the hub assembly and tower have not been modelled. The pitch of the blades and rotational speed of each of the rotors is constant, such that the downwind rotor does not compensate in any way for the reduction in torque available as a result of interaction. Whilst this may not be entirely representative of turbine operation in practice, it is essential to understand the fluid dynamics associated with wake impingement before adding the complication associated with the turbine control system. For a detailed description of the blade geometry, see Hand *et al.*;[19] the key properties of the turbine rotors are summarized in Table I, however. Unless otherwise stated, all of the data presented in this paper have been obtained from simulations in which the wake was discretized using a grid cell density of 20 cells per rotor radius and a blade that was modelled using 20 aerodynamic control points forming a cosine distribution along the length of the blade, such that control points are concentrated towards the root and tip of each blade.

The effect of the wake created by a reference rotor on the performance of a second turbine rotor placed downwind has been investigated over a range of rotor separations and different wind conditions. The rotor system is simulated in axial wind conditions at tip speed ratios of six and eight. Four different values for the downwind separation between the rotors were used: 4, 8, 12 and 16 rotor radii, according to the conventions defined in Figure 1. In addition, the interaction between two rotors that are separated by four rotor radii in the downwind direction were simulated with two different crosswind offsets between the axes of rotation of the rotors. In all cases, the rotors all rotate in the same direction, but in addition, a simulation was performed in which the downwind rotor rotates in the opposite sense to the reference rotor. In this simulation, the rotors were separated by four rotor radii and subjected to a wind giving a tip speed ratio of six. A list of the configurations that were simulated is given in Table II.

**Table I.** Rotor data.

| | |
|---|---|
| Type of rotor | Rigid |
| Number of blades | 3 |
| Rotor radius | R |
| Aerofoil | NREL S809 |
| Rotational speed | Ω (constant) |
| Blade tip pitch | 3° |

**Table II.** Simulated configurations and operating conditions.

| $\lambda$ | $x_h$ | $y_h$ |
|---|---|---|
| 6 | 4R | 0 |
| 6 (reverse rotation) | 4R | 0 |
| 6 | 8R | 0 |
| 6 | 12R | 0 |
| 6 | 16R | 0 |
| 7 | 4R | 0 |
| 8 | 4R | 0 |
| 8 | 4R | 1R |
| 8 | 4R | 2R |
| 8 | 8R | 0 |
| 8 | 12R | 0 |
| 8 | 16R | 0 |

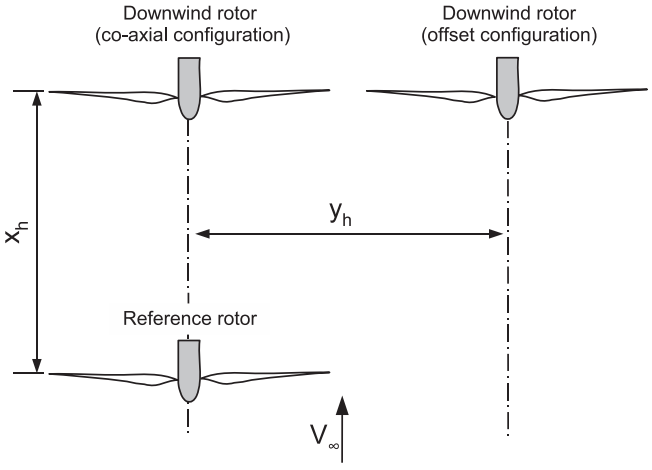


**Figure 1.** Relative locations of simulated wind turbine rotors.


*Wind Energ.* 2010; **13**:587–602 © 2009 John Wiley & Sons, Ltd.
DOI: 10.1002/we

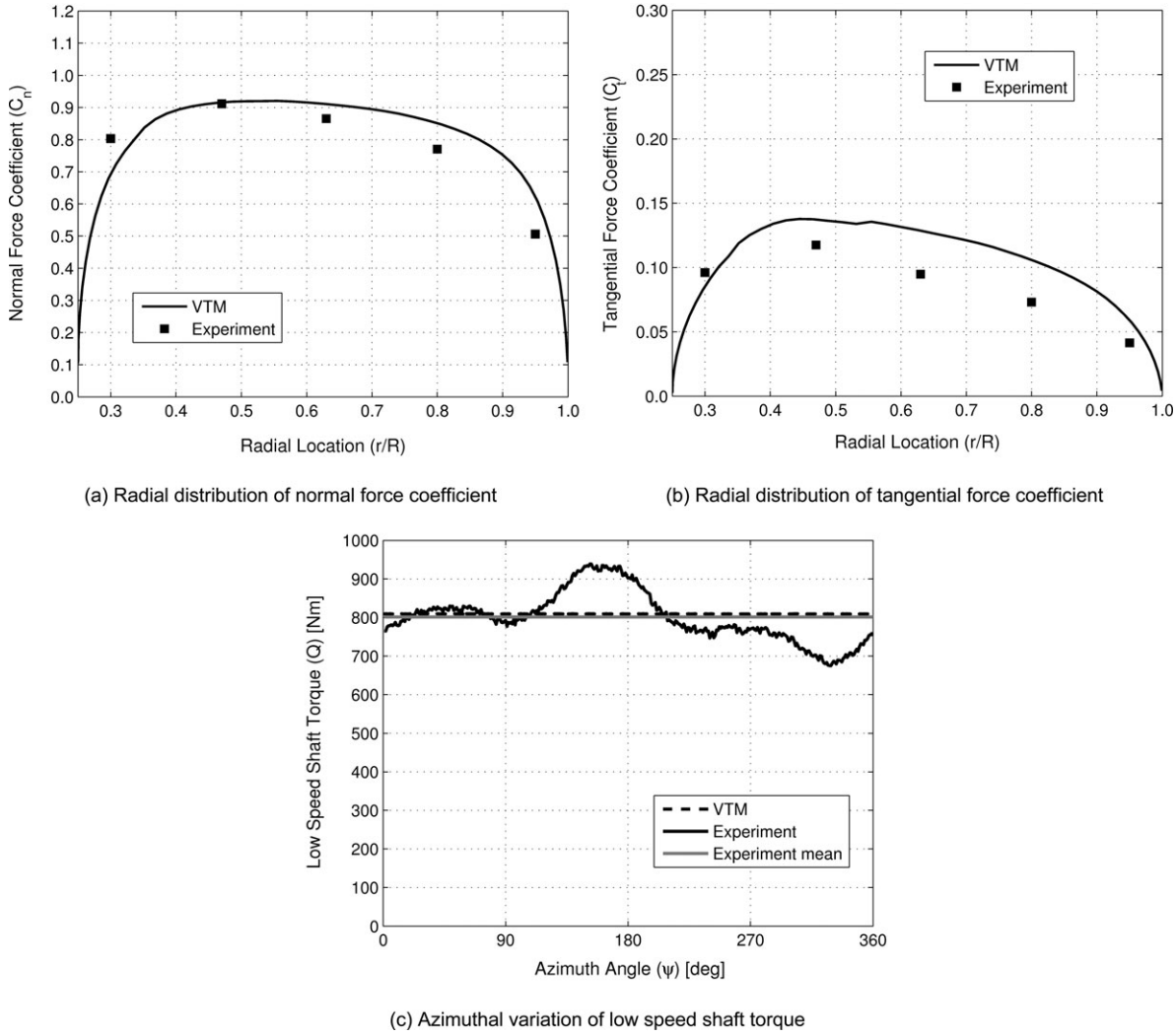


(a) Radial distribution of normal force coefficient

(b) Radial distribution of tangential force coefficient

(c) Azimuthal variation of low speed shaft torque

**Figure 2.** HAWT aerodynamic performance, computed using the VTM, compared with data from Phase VI of the NREL Unsteady Aerodynamics Experiment. $\lambda = 5.4$ ($V_\infty = 7$ m s$^{-1}$).

## 4. VERIFICATION OF AERODYNAMIC PREDICTIONS

Before investigating the effect of aerodynamic interaction on the performance of horizontal axis wind turbines, it is essential to first establish that the requisite fluid dynamic features within the flow surrounding the turbine rotor, and hence the aerodynamic loads on the blades of the rotor, are correctly simulated by the VTM. Figure 2 shows comparisons of the normal force coefficient, the tangential force coefficient and the low speed shaft torque predicted by the VTM with equivalent data obtained during Phase VI of the NREL Unsteady Aerodynamics Experiment.[19] The Phase VI rotor was mounted upwind of the tower, and operated in a wind of speed 7m/s (translating into a tip speed ratio of 5.4) at a yaw angle of zero. The data presented in Figure 2(a),(b) represent the mean values of the normal and the tangential force coefficients over one complete revolution with the rotor operating at an approximately constant rotational speed and, therefore, in a quasi-steady state.

Figure 2(a) shows that the magnitude of the normal force coefficient along most of the blade is predicted reasonably well by the lifting-line type blade model that is implemented within the VTM. The normal force coefficient is, however, over-predicted along the outboard third of the blade. The radial distribution of tangential force coefficient is slightly less well predicted by the VTM, as shown in Figure 2(b). In the past, considerable variations have been noted in measurements of the aerodynamic performance of aerofoils with identical definitions that have been tested in different wind tunnels. This uncertainty in the two-dimensional aerofoil data, and in particular the sectional drag coefficient data, along with the limitations

placed on predicting the centrifugal effects within the boundary layer inherent in the quasi-two-dimensional model of the blade aerodynamics, is thought to be largely responsible for the disparity in the aerodynamic loading on the blades. It should be noted, however, that of most relevance to the current work is the accuracy with which the VTM can predict the torque delivered to the shaft of the turbine rotor. In Figure 2(c), it can be observed that whilst the VTM does not replicate the unsteadiness in the shaft torque with the rotation of the rotor as the effects of tower interference and atmospheric turbulence, for example, were not modelled, the mean torque is very well predicted. Indeed, if the experimental data is averaged over the complete revolution shown, the magnitude of the shaft torque collapses almost exactly onto the steady value that is computed using the VTM.

The model of the blade aerodynamics that is implemented within the VTM uses a look-up table of aerofoil data that is assembled from experimental measurements, based on local angle of attack, to obtain the aerofoil lift, drag and pitching moment at each blade section. The best predictions of the aerodynamic loading on the wind turbine blades are thus obtained when the flow is almost entirely attached and is aligned with the chord of the blade; in other words, when the angle of attack at each blade section is sufficiently low that the blade operates within the linear aerodynamic regime. The VTM, along with many other aerodynamic tools that use relatively simple lifting-line type models for the blade aerodynamics, provides the most accurate predictions of the power produced by the wind turbine at high tip speed ratio. It is for this reason that tip speed ratios near the higher end of the realistic range for the type of rotor that was simulated were selected for investigation.

# 5. INTERACTION IN CO-AXIALLY ALIGNED TURBINES

The basic effects of aerodynamic interaction between two rotors are most readily exposed in a study of the couplings within a system in which the reference and downwind rotors are co-axially aligned and the incident wind is parallel to the shared axis of rotation of the turbines. Whilst in practice, wind farms are composed of a much larger number of turbines and, in addition, the disc tilt, orientation and wind conditions to which real turbines are subjected means that they are never entirely co-axial, both of these factors constitute necessary simplifications that enable the fundamental characteristics of wind farm interactions to be exposed.

## 5.1. Rotor performance

The generation of lift and drag forces on the rotor blades results in a momentum deficit within the wake that develops downwind of the turbine. When a second turbine is subject to direct impingement by the wake of an upwind rotor, the effective wind velocity that it experiences is reduced compared to that incident on the upwind rotor. The reduced flow speed manifests as a reduction in the power that may be extracted from the wind by the downwind turbine.

Figure 3 shows VTM predictions of the power coefficient developed by turbine rotors located at various distances downwind of a reference rotor, and demonstrates that the reduction in the mean power coefficient of the downwind rotor is strongly dependent on the wind speed and on the separation between the two rotors. When the reference rotor operates at a tip speed ratio of six, the

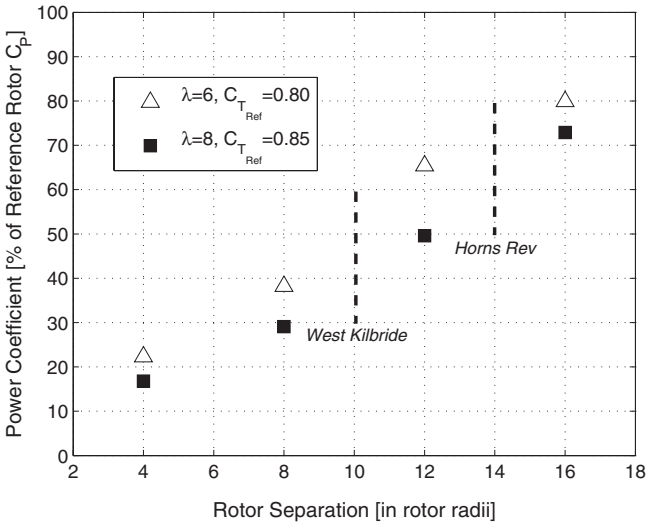


**Figure 3.** Power coefficient of the downwind turbine (as a percentage of the power coefficient of the reference rotor) as a function of the separation between the rotors for two different tip speed ratios of the reference rotor.


*Wind Energ.* 2010; **13**:587–602 © 2009 John Wiley & Sons, Ltd.
DOI: 10.1002/we

rotor positioned four rotor radii downwind develops only 22% of the power coefficient of the reference rotor. As the spacing between the rotors is increased, the power coefficient of the downwind rotor recovers in a non-linear fashion as the adverse effect of the interaction between the rotors is reduced. If the tip speed ratio of the reference rotor is increased to eight (equivalent to a reduction in wind speed) then the aerodynamic performance of the downwind rotor is degraded further, indicating that the adverse effects of aerodynamic interaction should increase in severity at lower wind speeds. The recovery in the power coefficient of the downwind rotor with increased separation between the rotors follows a very similar trend at both of the tip speed ratios that have been simulated, suggesting that a simple semi-empirical model may be capable of reproducing the variation of power output with turbine separation shown in Figure 3. The development of this model is complicated, however, by its reliance on a reduced-order theory to describe the downstream variation of the mean velocity within the turbine wake, particularly in the presence of the vortex instabilities that will be shown in the following section of the paper to have a key influence on the performance of the downwind turbine.

Figure 4(a),(b) show the variation in the power coefficient developed by the reference and downwind rotors operating in axial wind conditions at tip speed ratios of six and eight, respectively, over the entire time period over which each of the rotors have been operated following start-up. The power coefficient of both the reference and downwind rotors undergoes a transient overshoot following the impulsive start-up of the rotor at the beginning of each simulation. Once the initial transient loads have subsided, the reference rotor continues to develop an almost constant power coefficient as a result of its operation within a uniform and steady incident wind, unperturbed by impingement from the wake of other rotors. The separation between the reference and downwind rotors is sufficiently large that the aerodynamic performance of the reference rotor is not affected by the presence of the downwind rotor. The initial impingement of the wake of the reference rotor results in a period of time during which the power absorbed by the downwind rotor fluctuates considerably. The transient unsteadiness in the power developed by the

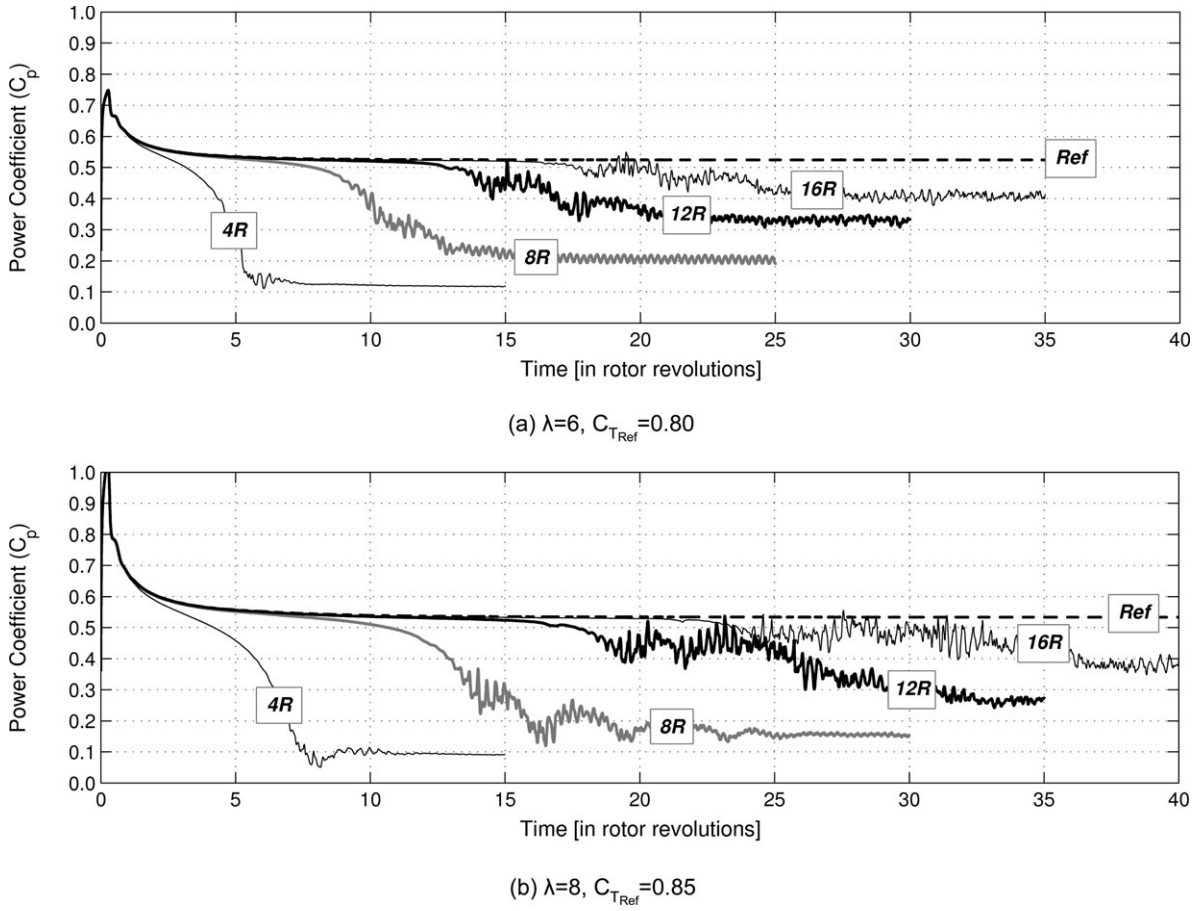


**Figure 4.** Reduction in power coefficient as a function of time after an instantaneous start, for rotors located 4, 8, 12 and 16 rotor radii downstream of the reference rotor (Ref: reference rotor).

downwind rotor is more persistent the greater the spacing between the reference and downwind rotors, as can be seen by comparing the variations in power coefficient presented in Figure 4. This transient performance results directly from the fluctuations in the induced velocity at the downwind rotor that follow the breakdown of the wake that is developed by the reference rotor into finer scale vortical structures, as is shown in the next section of this paper.

The reduction in the power coefficient developed by the downwind rotor is, of course, the result of this rotor developing a driving torque which is lower than that developed by the reference rotor. Figure 5(a),(b) show the time-averaged radial distribution of normal force coefficient, at tip speed ratios of six and eight, respectively, developed by the rotors represented in Figure 3 once quasi-steady-state conditions are reached. It is clear that the power coefficient developed by a rotor operating within the wake of another is reduced as a result of its blades developing an aerodynamic loading that is significantly lower than that which is generated on the blades of the rotor when operated in isolation. Indeed, the aerodynamic performance of the blades of the downwind rotor is lower than that of the reference rotor along their entire length. This indicates that the downwind rotor as a whole is adversely affected by aerodynamic interaction with the wake of the reference rotor, as is to be expected given the geometry of the wake, as shown in the next section. The results suggest that the relative reduction in normal force coefficient along the length of the blades of the downwind rotor, when compared to the reference rotor, is somewhat larger when the rotors operate at a higher tip speed ratio.

The reduction in the mean power coefficient of the downwind rotor is largest when the spacing between the downwind and reference rotors is smallest. However, the unsteadiness in the power coefficient of the downwind rotor is greatest when the rotors are separated by the largest

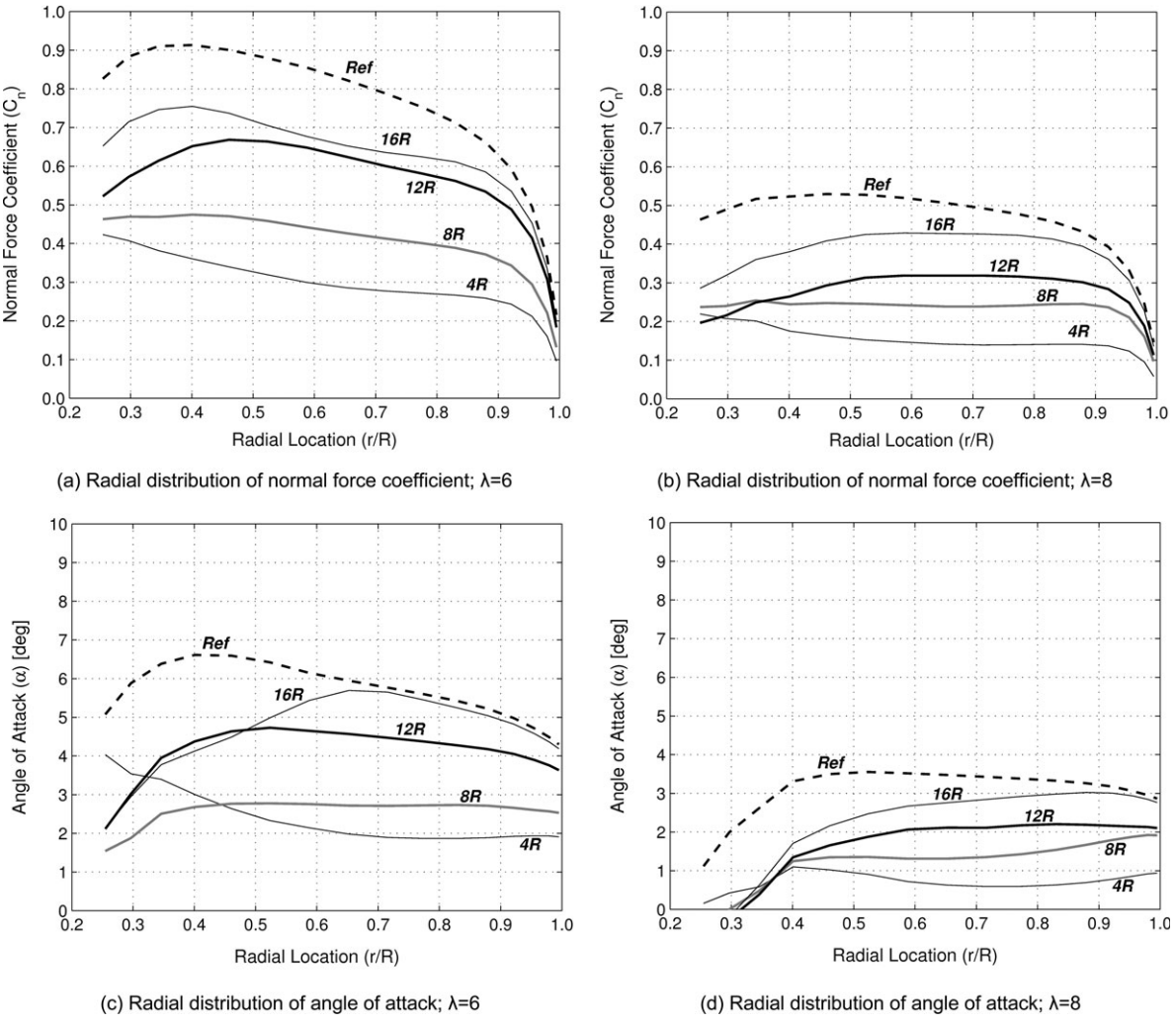


**Figure 5.** Variation in the aerodynamic loading on axially co-aligned rotors as a function of the separation between the rotors for two different tip speed ratios of the reference rotor (Ref: reference rotor).



*Wind Energ.* 2010; **13**:587–602 © 2009 John Wiley & Sons, Ltd.
DOI: 10.1002/we

distance, as shown in Figure 4(a),(b). The amplitude of the fluctuations in the normal force coefficient that occurred over the duration of each revolution were relatively small and, therefore, indicate that the trends shown in Figure 5 are representative of the downwind rotor operating at a quasi-steady-state. The distributions of normal force coefficient shown in Figure 5(a),(b) are consistent with the associated variation of angle of attack along the length of the blades shown in Figure 5(c),(d). The relative reduction in the angle of attack along the blades with the separation between the rotors is larger at the higher of the two tip speed ratios, as is shown by a comparison of Figure 5(c),(d). Indeed, as the separation between the rotors is increased, the distribution of angle of attack along the blades of the downwind rotor recovers more quickly to that on the blades of the reference rotor when the tip speed ratio at which the rotors operate is lower. This suggests that as the wind speed in which the rotors operate is increased, the adverse effect on the power that is generated by the downwind turbine rotor as a result of wake interaction is reduced.

## 5.2. Structure of the flow field

The aerodynamic performance of a rotor positioned downwind of a second rotor is strongly influenced by the wake of the upwind rotor. Indeed, the effect on the power coefficient of the downwind rotor that is demonstrated in Figure 3 indicates the substantial influence that the velocity that is induced by the upwind rotor has on the performance of the downwind rotor. Figure 6 shows the characteristic features of the wake system surrounding the reference and downwind rotors for three rotor separations (4R, 8R and 12R) and with the reference rotor operating

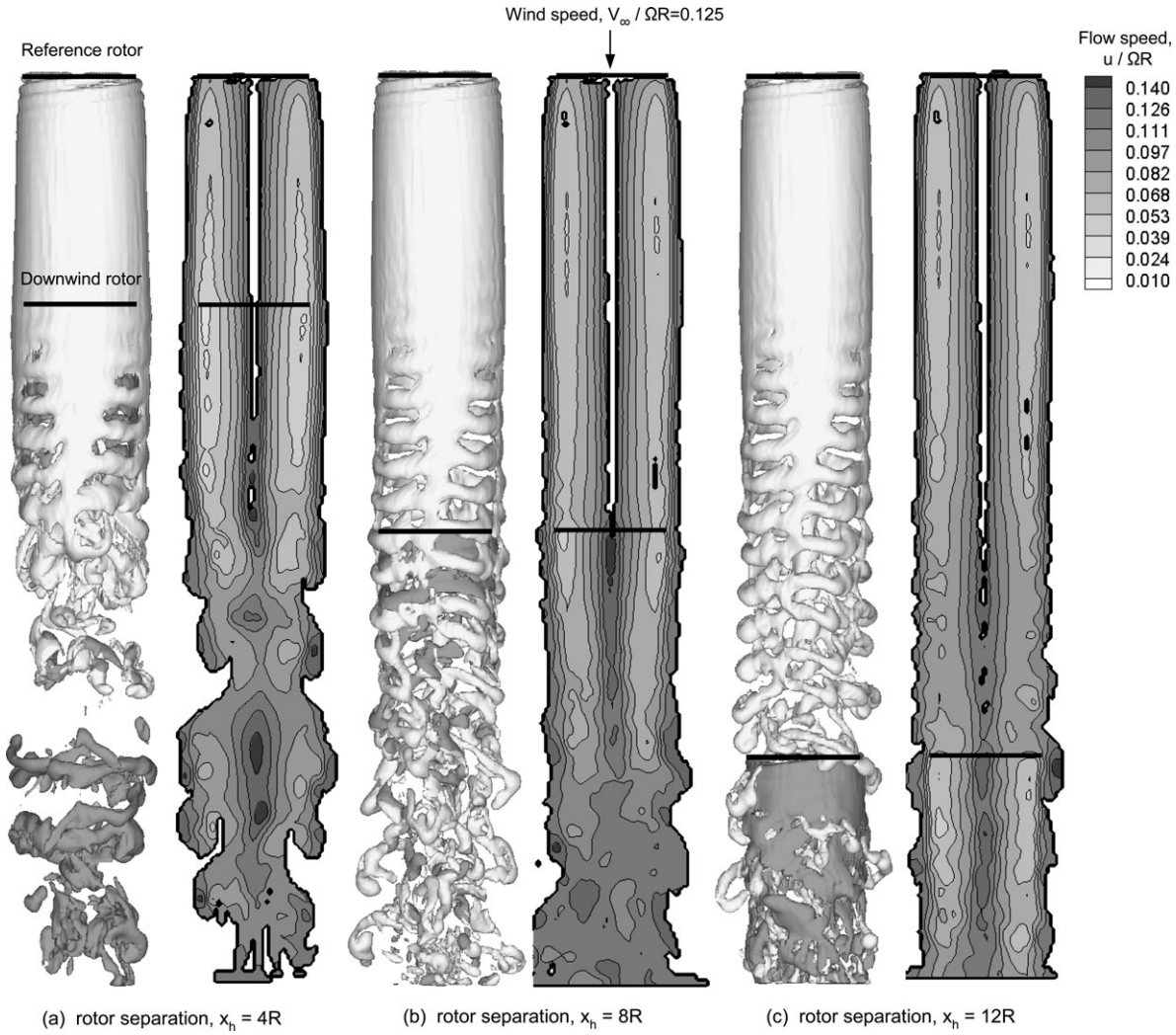


**Figure 6.** Vorticity and velocity distributions in the flow surrounding two co-axially aligned rotors. $\lambda = 8$, $C_{T_{Ref}} = 0.85$. At left of each sub-figure: instantaneous iso-surface of vorticity representing the wake (light grey: reference rotor, dark grey: downwind rotor). At right of each sub-figure: contours of flow speed normalized using the rotor tip speed.

at a tip speed ratio of eight. To the left of each sub-figure is an instantaneous snapshot of the three-dimensional wake structure. The wake is represented by plotting a surface of constant vorticity magnitude in the flow. To the right of each sub-figure, a contour map is plotted showing the distribution of flow speed (velocity magnitude) within the wake system.

Figure 6 shows that the helical structure developed by the tip vortices from a rotor operating at a high tip speed ratio persists for a relatively limited distance downwind of the rotor. The products of the natural instabilities within the wake, that manifest first as local pairing and leap-frogging of the vortex filaments,[17] develop with time to form larger aperiodic vortex structures. The impingement of the wake created by the reference rotor on the downwind rotor further promotes the development of disturbances within the wake, augmenting those already present within the wake of the reference rotor. This leads to the breakdown of the structure of the combined wake system of the two rotors, as shown in Figure 6(a). The relatively light loading on the blades of the downwind rotor when positioned a relatively short distance downwind of the reference rotor necessarily limits the vorticity trailed from that rotor into the wake. As the spacing between the rotors is increased, a coherent and quasi-periodic vortical structure is able to persist to a greater distance downwind of the reference rotor before being disrupted by the impingement of the wake on the downwind turbine, as is indicated by a comparison of the instantaneous snapshots of vorticity shown in Figure 6(a),(c). If the tip speed ratio at which the rotor operates is lower (equivalent to a higher wind speed), the helical structure formed by the concentrated tip vortices persists to greater distances downwind since in this case the wake is convected more rapidly by the freestream component of the flow.

Figure 6 illustrates why a re-formulation of blade element momentum theory (BEMT), as has been suggested in some quarters, in order to model the performance of the downwind rotor within the wake of the reference rotor is, in fact, inappropriate, especially where a substantial distance exists between the two rotors. Versions of the BEMT have been developed for co-axial helicopter rotors operating in hover, and the temptation might arise to formulate a co-axial wind turbine BEMT for the windmill brake state. If a similar approach was applied to the aerodynamic interaction between two wind turbine rotors, the power deficiency of the downwind rotor would asymptote to a constant value as the separation between the rotors is increased and hence as the downwind rotor is moved into the fully-expanded portion of the idealized wake. If this analysis were to be applied to wind turbines that are separated by a distance typical of current wind farms (as an indication, 10–16 rotor radii), the aerodynamic performance of the downwind rotor would become insensitive to the separation between the reference and downwind rotors. This result would clearly be at odds with the variation in power coefficient that is shown in Figure 3 and the distribution of flow speed within the wake downwind of the reference rotor that is demonstrated by a comparison of Figure 6(a)–(c).

The instantaneous snapshots of the wakes of the reference and downwind rotors, shown in Figure 6, were calculated using a relatively coarse computational grid. In order to understand better the detailed dynamics of vortical structures within the flow field near to the rotors as they convect downwind, it is necessary to visualize the wake of the rotor system at significantly finer scales. This is achieved by simulating the flow around the rotor system using a significantly higher density of cells within the computational domain (50 cells per rotor radius) and an associated increase in the number of aerodynamic control points along the length of the blades to 50. Figure 7 shows contours of the magnitude of the vorticity within the wakes developed by both the reference and downwind rotors that were computed using a high-resolution simulation. In order to be representative of the fluid dynamics within the wakes of the configurations simulated in this paper, the rotors shown in Figure 7 are separated by a distance of four rotor radii and operate at a tip speed ratio of seven. The individual trailed vortices that form downwind of the roots and the tips of the blades, along with the sheet of vorticity that is shed from the trailing edge of each blade, can be observed clearly downwind of the reference rotor. At a distance of approximately 1–2 radii downwind of the reference rotor, vortex pairing and leap-frogging instabilities develop in the tip vortices and result in an aperiodic wake structure by the time the vorticity reaches the downwind rotor. As the vortices that are trailed from the roots and tips of the blades of the upstream rotor impinge on the downwind rotor, they interfere with the development of the helical wake structure of the downwind rotor, and can be contrasted with the region of the downwind rotor wake, as shown in Figure 7, that is, as yet, undisturbed by interaction with the wake developed by the reference rotor. Figures 6 and 7 demonstrate the significant effect of both the stability and the dynamics of the wake of the reference rotor on the performance of any rotor located downwind. Indeed, it is clear that the velocity deficit at the downwind rotor and, therefore, the aerodynamic coupling between the rotors in a wind farm, is governed significantly by the inviscid process of wake breakdown that occurs because of the natural instability of the vortices within the wake. The results presented here suggest that the viscous dissipation that occurs at very fine scales within the wake may indeed have only a relatively minor influence on the performance of the downwind rotor.

## 6. INTERACTION BETWEEN TURBINES WITH OFFSET ROTOR AXES

The majority of the aerodynamic interactions within wind farms occur when the turbines are operating ‘off-design’. This follows from the practice of designing the orientation and spacing of the turbines within a farm to minimize


*Wind Energ.* 2010; **13**:587–602 © 2009 John Wiley & Sons, Ltd.
DOI: 10.1002/we

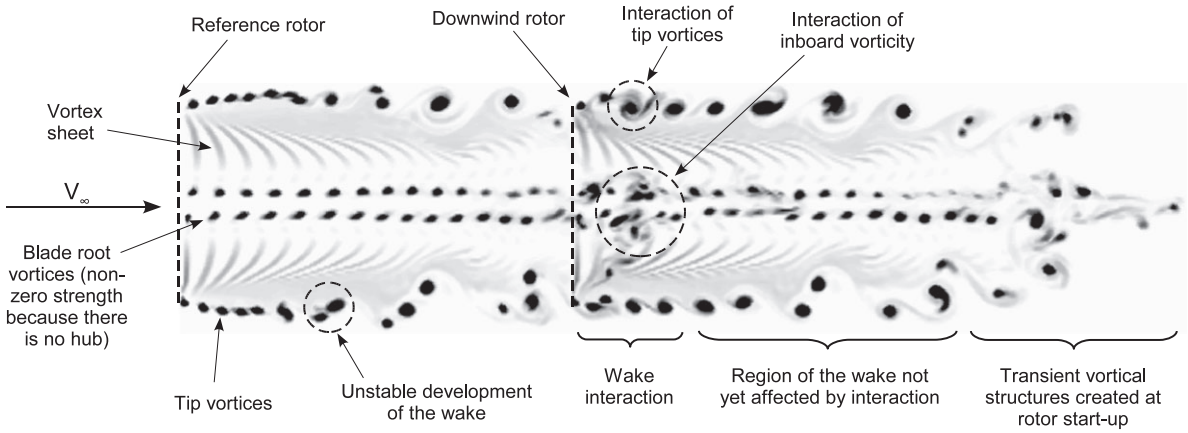


**Figure 7.** The characteristics of the wake of two interacting wind turbine rotors. The wake is represented using contours of vorticity magnitude on a plane through the reference and downwind rotors operating in a co-axial configuration. $x_h = 4R$, $\lambda = 7$.

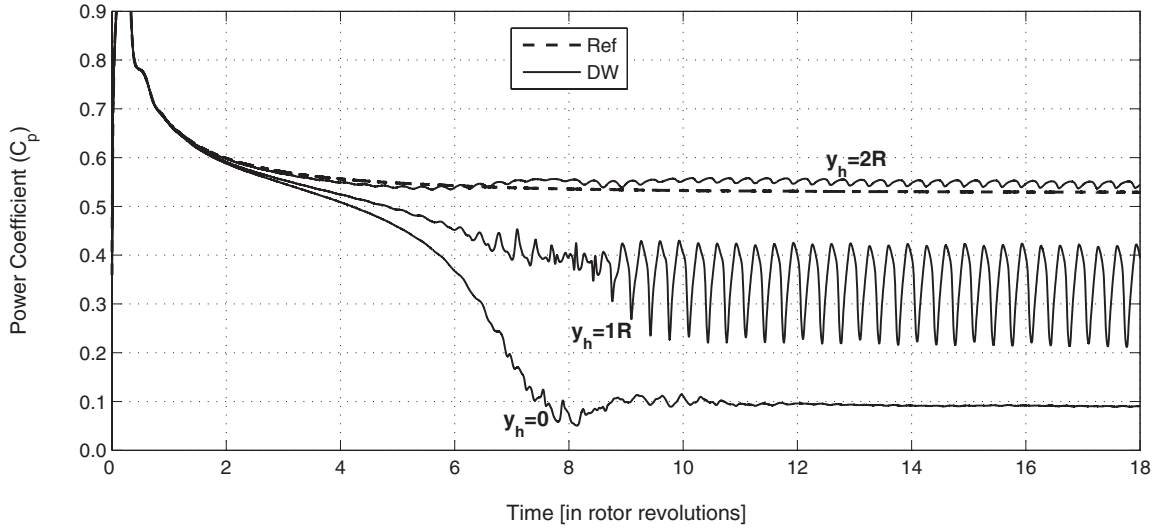


**Figure 8.** Effect of crosswind offset from the reference rotor on the power coefficient of the downwind rotor (Ref: reference rotor, DW: downwind rotor). $x_h = 4R$, $\lambda = 8$.

interactions when the wind is blowing in one specific direction, invariably taken to be the prevailing wind direction. The impingement of the wake generated by an upwind turbine on a second turbine that is located further downwind often affects only part of the downwind rotor disc. This form of asymmetric interaction can occur either because the turbines are offset in the crosswind direction, or because of the wind direction. Interactions where approximately half of the downwind rotor disc is affected by impingement from a wake generated upwind are sometimes referred to as 'half-wake' interactions, rather than the 'full-wake' interactions that would occur if two turbines were configured co-axially and operated within a wind that was parallel to their shared axis of rotation. Interactions in which there is only partial wake impingement on the downwind turbine can lead to large variations in the loading on the blades of this turbine as they rotate around the rotor azimuth. The ensuing oscillations in the forces and moments, on both the blades and the rotor hub, can reduce the fatigue life of the turbine.

Figure 8 shows the effect of crosswind offset from the reference rotor on the power coefficient of the downwind rotor. In each case, as with Figure 4 shown earlier, the data is presented from the initial starting of the rotor to the time at which the downwind rotor operates at a quasi-steady mean power coefficient. Indeed, it is worth noting that the short distance between the reference and downwind rotors results in the onset of interaction between the rotors after a few rotor revolutions have elapsed. The temporal variation of the power coefficient that is developed by the downwind rotor in the configuration with no separation between the axes of rotation of the reference and downwind rotors is reproduced in Figure 8 to facilitate comparison. It is clear from Figure 8 that the power coefficient

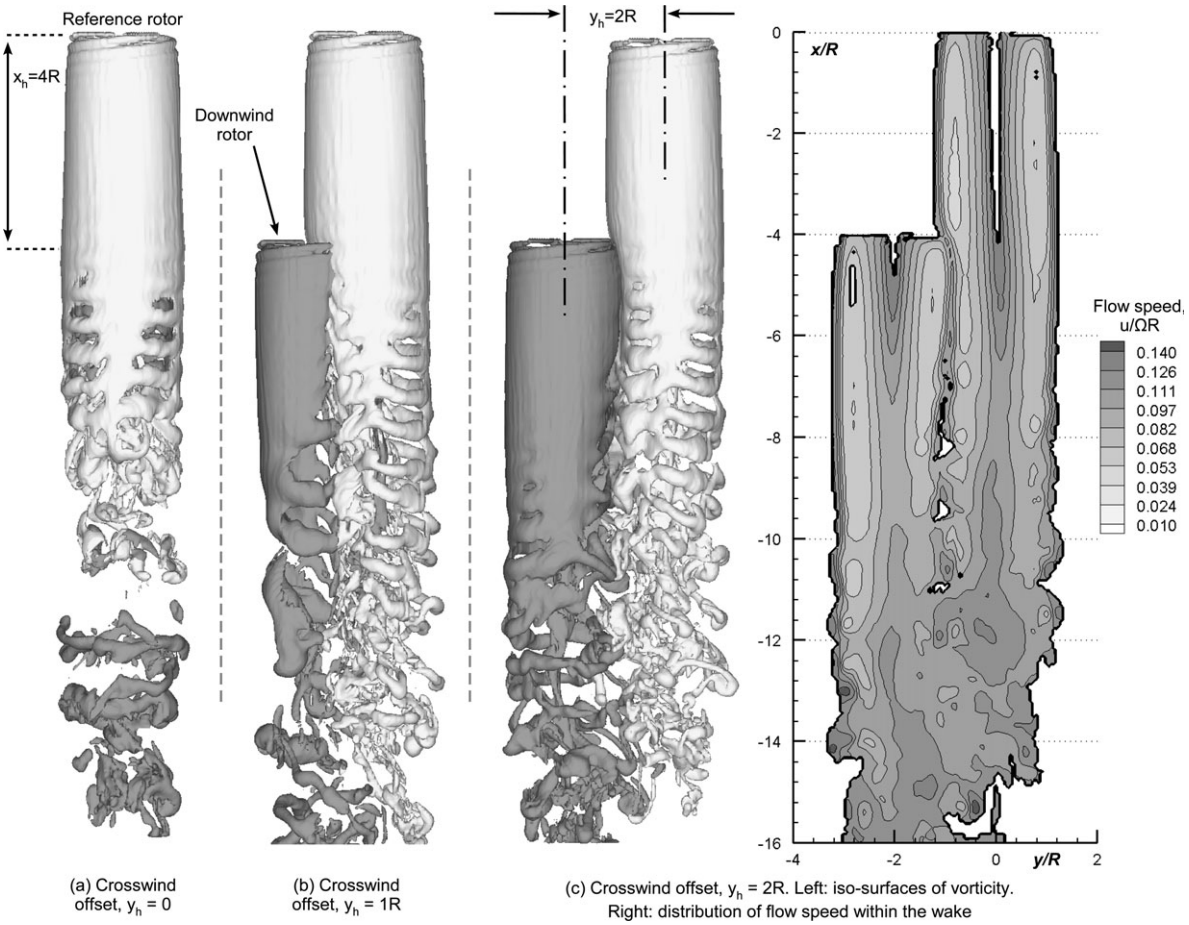


**Figure 9.** Instantaneous snapshots of the wake developed by the reference and downwind rotors operating with three different crosswind offsets. $x_h$ = 4R, $\lambda$ = 8.

developed by the downwind rotor that is offset in the crosswind direction by one rotor radius is higher than the power coefficient that is developed by the same rotor when configured with no crosswind offset.

The increase in the power coefficient of the downwind rotor as the crosswind offset between the turbines is increased to one rotor radius is, however, accompanied by the onset of significant unsteadiness in the performance of the downwind rotor. The unsteadiness occurs because the wake developed by the reference rotor impinges on approximately only half of the downwind rotor disc. This impingement is an example of a 'half-wake' interaction, and is illustrated by Figure 9(a),(b), which compare the wake structure that is developed by a system of interacting turbine rotors that are configured co-axially with a system where there is a crosswind offset of one rotor radius between the turbines. In Figure 9(a),(b), the wakes are represented using iso-surfaces of vorticity magnitude. The effect of the partial impingement of the wake developed by the reference rotor on the distribution of normal force coefficient on the downwind rotor can be seen by comparing Figure 10(a),(b), again, for the co-axial and offset configurations, respectively. Figure 11(a),(b) show the corresponding distributions of tangential force coefficient. In the rotor configurations simulated in this paper, the angle of attack is typically less than 10 degrees at each of the radial stations along the blades. As a result, the tangential force coefficient on the blades of the downwind rotor provides a significant component of the torque that drives the rotor. Indeed, even though the magnitude of the normal force coefficient is, in general, significantly greater than that of the tangential force, only a small component of the normal force acts to drive the rotation of the rotor. Figure 10(b) clearly illustrates the asymmetry in the normal force coefficient on the disc of the downwind rotor that results from its partial immersion within the wake of the reference rotor, as a large region of low aerodynamic loading that is present on the right-hand half of the rotor disc. Similar asymmetry may be observed in the distribution of tangential force over the disc of the downwind rotor, as shown in Figure 11(b).

The impingement of the reference rotor wake on the downwind rotor is largely, but not entirely, eliminated when the offset between the rotor axes of rotation is


*Wind Energ.* 2010; **13**:587–602 © 2009 John Wiley & Sons, Ltd.
DOI: 10.1002/we

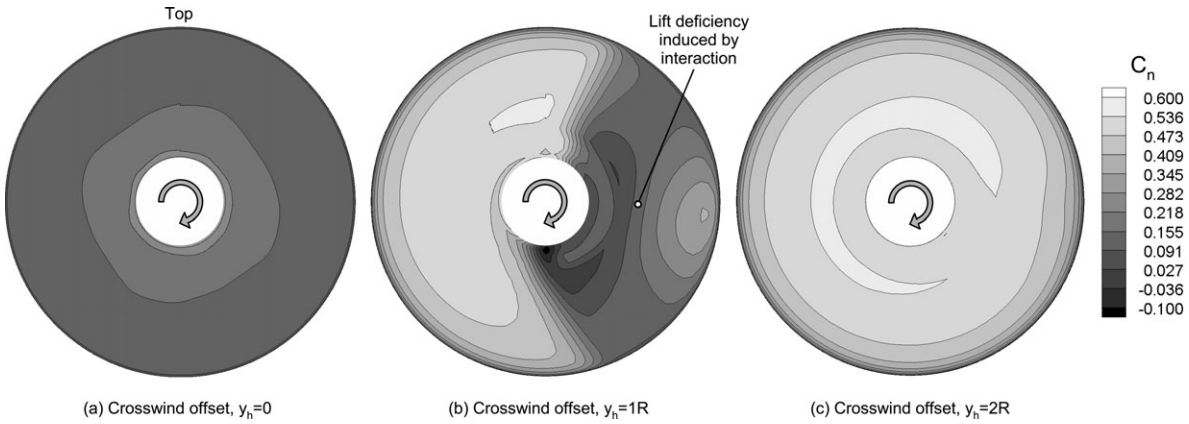


**Figure 10.** Distribution of blade normal force coefficient on the downwind rotor, during one complete revolution, when operating with three different crosswind offsets (viewed from the downwind side of the rotor). $x_h$ = 4R, $\lambda$ = 8.

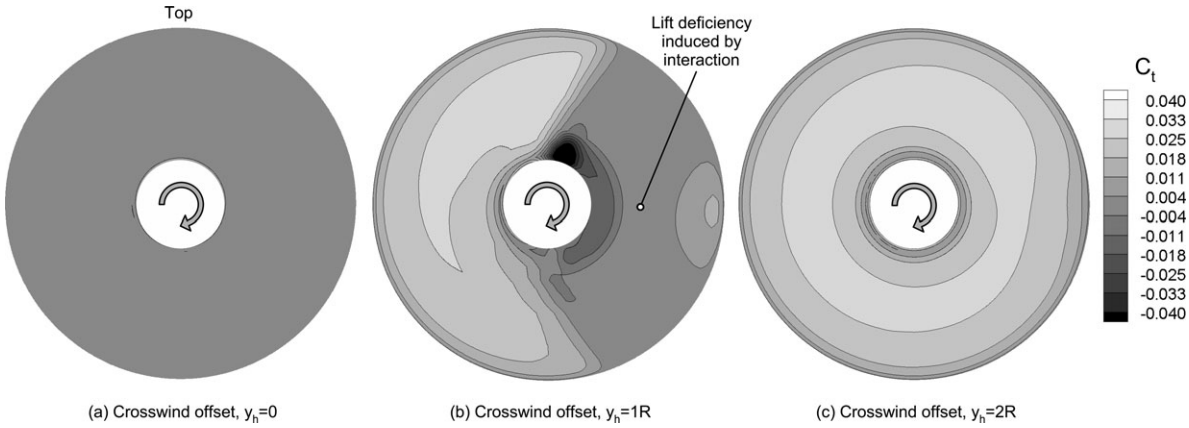


**Figure 11.** Distribution of blade tangential force coefficient on the downwind rotor, during one complete revolution, when operating with three different crosswind offsets (viewed from the downwind side of the rotor). $x_h$ = 4R, $\lambda$ = 8. A positive value of $C_t$ represents a driving force on the rotor.

increased to two rotor radii. The expansion of the wake that is developed by the reference rotor as a result of the reduction in the momentum of the flow across the reference rotor disc yields a limited interaction between the two turbines. In this configuration, the wake of the upwind rotor induces a mild change in the local wind velocity at the downwind rotor, yielding the small increase in its power coefficient that is shown in Figure 8. In Figure 9(c), the wakes developed by both the reference and downwind turbine rotors are represented using both iso-surfaces of vorticity and contours of the velocity magnitude. It is clear from Figure 9(c) that there is a mutual distortion of both the wake downstream of the reference rotor and the flow around the downwind rotor. The effect of this interaction on both the normal and the tangential force coefficients developed by the downwind rotor is demonstrated in Figures 10(c) and 11(c), respectively. The asymmetry in the aerodynamic loading on the downwind rotor disc, whilst modest, is sufficient to result in the small improvement in the overall performance of the rotor that is shown in Figure 8.

In practice, unsteadiness in the loading on the blades is detrimental to the fatigue life of the turbine. The results presented in Figure 4 indicate that of the four different streamwise rotor separations simulated in this paper, the unsteadiness resulting from aerodynamic interaction is most significant when the separation between the rotors is largest (in the current work, sixteen rotor radii). Furthermore, the unsteadiness in performance is exacerbated when the downwind rotor is only partially immersed within the wake induced by the reference rotor. These findings are of significant practical interest given that the turbines operating within wind farms are typically separated by 10–16 rotor radii, and will be subject to partial, rather than co-axial (or 'full-wake'), interactions throughout most of their useful life. It should be noted, however, that the unsteadiness in the power coefficient of the downwind rotor cannot continue to increase indefinitely for

rotor separations greater than those simulated for this paper. Indeed, the breakdown of structure within the wake as a result of its natural instability will ensure that a separation distance will be reached beyond which the effect of the reference rotor on the downwind rotor will be negligible.

## 7. THE EFFECT OF THE SENSE OF ROTOR ROTATION

It has been known for many decades that in certain flight conditions, the performance of the tail rotor of a helicopter with a single main rotor is highly sensitive to the sense of its rotation. This effect is most certainly a result of aerodynamic coupling between the main and tail rotors, but for many years, was not well understood. Recent studies have shown that the sensitivity of the performance of the tail rotor to its direction of rotation is related to the velocity distribution that is induced on the tail rotor by the impingement of the vortical structures that are produced by the wake of the main rotor.[14] These studies raise the question of whether the performance of a wind turbine may also be sensitive to its sense of rotation when it is aerodynamically coupled to the other turbines within a wind farm.

Figure 12 shows a comparison of the radial distributions of normal force coefficient and angle of attack as predicted by the VTM on rotors with opposing senses of rotation as they interact with a reference rotor mounted upstream. In the first case, the downwind rotor rotates in the same sense as the reference rotor, whilst in the second case, the downwind rotor rotates in the opposite sense to the reference rotor. The spacing between the rotors is four rotor radii and the tip speed ratio is six for both of the configurations shown in the figure. Figure 12(a) clearly shows that when the sense of rotation of the downwind rotor opposes that of the reference rotor, the downwind rotor develops a lower normal force coefficient over the inboard portion of the blade when compared to the downwind rotor that has the same sense of rotation as the reference rotor. The reduction in force developed on the blades can be attributed directly to a lower angle of attack along the blades, from the root cut-out to the 0.7R radial location, as shown in Figure 12(b).

Despite the marked differences in the performance of the blades shown in Figure 12, reversing the sense of rotation of the downwind rotor has only a very small effect on the power coefficient that it develops. The quasi-steady power coefficient of the downwind turbine that has the same sense of rotation to the reference rotor is 0.117 compared with 0.109 for the downwind turbine with the opposite sense of rotation. It should be remembered, however, that the relationship between the aerodynamic loading on particular portions of the blades and the power coefficient of the rotor is far from straightforward. Indeed, the rotor is driven only by those blade sections at which the forward component of the lift is large enough to overcome the profile drag, and therefore where the rotor absorbs energy from the wind. Figure 12(a) suggests, nevertheless, that the loads that are developed on aerodynamically coupled turbine rotors within wind farms can be, to some extent, influenced by the relative sense of rotation of the turbine rotors. It should be borne in mind, however, that the current turbine model does not account for the presence of a hub, transmission assembly, or tower. In addition, the turbulence that is ordinarily present within the incident wind, and that has not been modelled in the present study, would modify the vortex system that is created behind the blades of each turbine. In practice, therefore, the vortices trailed from the roots of the blades would possess neither the same strength nor coherence as those computed in the present study. Instead, a highly unsteady and disordered

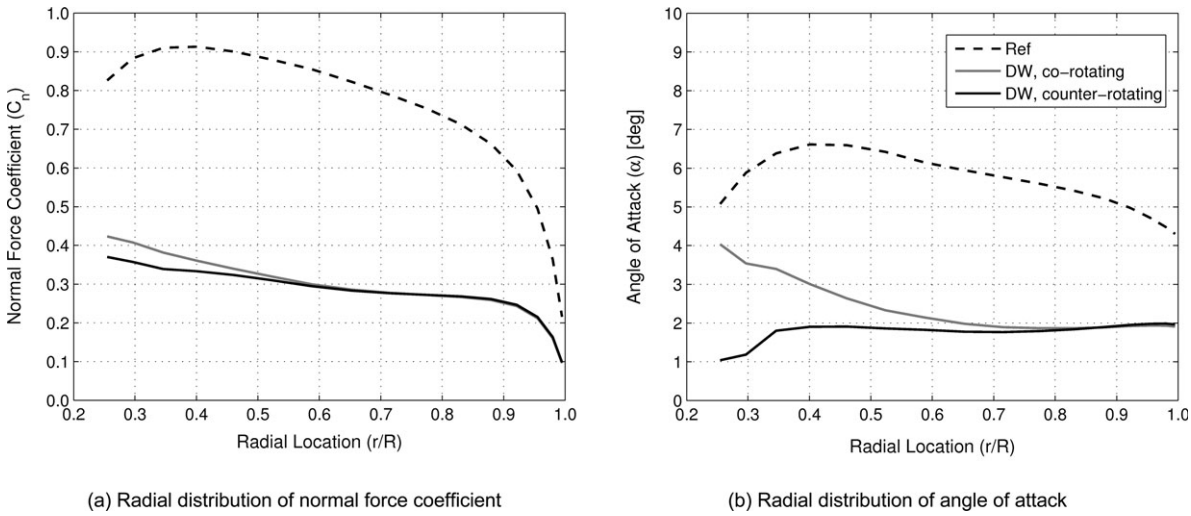


(a) Radial distribution of normal force coefficient

(b) Radial distribution of angle of attack

**Figure 12.** Effect of sense of rotation on the distribution of normal force coefficient and angle of attack along the blades of the downwind rotor (Ref: reference rotor, DW: downwind rotor). $x_h = 4R$, $\lambda = 6$, $C_{T_{Ref}} = 0.80$.



*Wind Energ.* 2010; **13**:587–602 © 2009 John Wiley & Sons, Ltd.
DOI: 10.1002/we

wake would form downwind of the multiple elements that compose the rotor hub. These additional features may have a significant effect on the results presented in Figure 12. The results presented in Figure 12 do, nevertheless, indicate that whilst the sensitivity of the performance of the downwind rotor to its direction of rotation is relatively modest in the present simulations, further work should be undertaken using a more realistic model of the blade root in order to expose the true benefits, if any, of reversing the sense of rotation with respect to the reference rotor.

## 8. CONCLUSION

The aerodynamic interaction between wind turbines operating in axial wind conditions has been simulated in order to understand better how the power coefficient of wind turbine rotors is influenced by the detailed structure of the wake generated by a rotor located further upwind. In particular, the aim has been to expose the role of vortex instability in governing the structure of the wake at significant distances downstream of the rotor, where further turbines may be located within a wind farm. The dependence on tip speed ratio, both the streamwise and crosswind separation between the rotors, and the sense of rotation of the downwind rotor with respect to the rotor located further upwind of the power output of a wind turbine rotor that is subject to aerodynamic interaction with the wake of another turbine has been investigated.

A rotor located downwind of another suffers a reduction in its aerodynamic power output if subject to impingement by the wake of the upstream rotor. Less power is lost as the separation between the rotors is increased, but the simulations performed in this paper suggest that rotors located even 12 radii apart may experience a 40–50% reduction in power for tip speed ratios in the range 6–8. The power coefficient developed by the downwind rotor, as a fraction of its performance in an undisturbed wind, reduces as the tip speed ratio of the rotors increases. If a crosswind offset is present between the respective axes of rotation of the reference and downwind rotors, significant unsteadiness can be present in the power coefficient developed by the downwind rotor. This unsteadiness in performance results from the asymmetry that is created in the normal and tangential components of force on the blades when subject to a highly asymmetric interaction with the wake induced by the reference rotor. The aerodynamic loading on the inboard portion of the blades of a wind turbine rotor interacting with another rotor that is located upwind, appears, to some extent, to be sensitive to the direction in which the downwind rotor rotates with respect to the upwind rotor. The evolution of the wake of the upstream turbine plays a critical role in governing the power that is developed by rotors located further downwind. The primary effect of interaction with the wake of the upstream rotor is to reduce the local wind speed at the downwind rotor. Crucially, however, the natural instability of the turbine wake acts to moderate the deficit in wind speed at the downwind rotor and, as the distance between the rotors is increased, the breakdown of structure within the wake of the reference rotor allows a recovery in the performance of the downwind rotor.

The results presented in this paper thus contribute to an understanding of the aerodynamic origin of the adverse effects on the performance of a wind farm that may be expected by increasing the density of its constituent turbines. Indeed, the growth of the wind energy industry, particularly in terms of onshore developments, will be accompanied by increasing constraints on the availability of space for turbines and will therefore rely increasingly on the efficient utilization of suitable sites. As such, it is hoped that the numerical techniques and results described in this paper will be of use to the developers of wind farms in helping to reduce the inefficiencies in performance and the uncertainty in power yields that arise from aerodynamic interactions between the individual turbines that constitute the farm.

## REFERENCES

1. Vermeer LJ, Sørensen JN, Crespo A. Wind turbine wake aerodynamics. *Progress in Aerospace Sciences* 2003; **39**:467–510.
2. Crespo A, Hernández J, Frandsen S. Survey of modelling methods for wind turbine wakes and wind farms. *Wind Energy* 1999; **2**:1–24.
3. Newman BG. The spacing of wind turbines in large arrays. *Energy Conservation* 1977; **16**:169–171.
4. Builtjes PJH, Smit J. Calculation of wake effects in wind turbine parks. *Wind Engineering* 1978; **2**:135–145.
5. Lissaman PBS. Energy effectiveness of arbitrary arrays of wind turbines. *Journal of Energy* 1979; **3**:323–328.
6. Milborrow DJ. The performance of arrays of wind turbines. *Journal of Wind Engineering and Industrial Aerodynamics* 1980; **5**:403–430.
7. Sforza PM, Sheering P, Smorto M. Three-dimensional wakes of simulated wind turbines. *AIAA Journal* 1981; **19**:1101–1107.
8. Voutsinas SG, Rados KG, Zervos A. On the analysis of wake effects in wind farms. *Wind Engineering* 1990; **14**:204–219.
9. Barthelmie RJ, Frandsen ST, Rathmann O, Hansen K, Politis ES, Prospathopoulos J, Cabezon D, Rados K, van der Pijl SP, Schepers JG, Schelez W, Phillips J, Neubert A. Flow and wakes in large wind farms in complex terrain and offshore. *European Wind Energy Conference*, Brussels, Belgium, 31 March–3 April, 2008.

10. Troldborg N, Sørensen JN, Mikkelson R. Actuator line simulation of wake of wind turbine operating in turbulent inflow. *Journal of Physics: Conference Series* 2007; **75**:012063.
11. Brown RE. Rotor wake modeling for flight dynamic simulation of helicopters. *AIAA Journal* 2000; **38**:57–63.
12. Brown RE, Line AJ. Efficient high-resolution wake modeling using the vorticity transport equation. *AIAA Journal* 2005; **43**:1434–1443.
13. Toro EF. A weighted average flux method for hyperbolic conservation laws. *Proceedings of the Royal Society of London, Series A: Mathematical and Physical Sciences* 1989; **423**:401–418.
14. Fletcher TM, Brown RE. Main rotor—tail rotor interaction and its implications for helicopter directional control. *Journal of the American Helicopter Society* 2008; **53**:125–138.
15. Kenyon AR, Brown RE. Wake dynamics and rotor-fuselage aerodynamic interactions. *Journal of the American Helicopter Society* 2009; **54**:012003.
16. Green RB, Gillies EA, Brown RE. The flow field around a rotor in axial descent. *Journal of Fluid Mechanics* 2005; **543**:237–261.
17. Ahlin GA, Brown RE. Wake structure and kinematics in the vortex ring state. *Journal of the American Helicopter Society* 2009; **54**:032003.
18. Kim HW, Brown RE. Coaxial rotor performance and wake dynamics in steady and manoeuvring flight. *62nd American Helicopter Society Annual Forum*, Phoenix, Arizona, USA, 9–11 May 2006.
19. Hand MM, Simms DA, Fingersh LJ, Jager DW, Cotrell JR, Schreck S, Larwood SM. Unsteady aerodynamics experiment phase vi: wind tunnel test configurations and available data campaigns. *NREL Report TP-500-29955*, 2001.



*Wind Energ.* 2010; **13**:587–602 © 2009 John Wiley & Sons, Ltd.
DOI: 10.1002/we